Draft version May 12, 2021
Typeset using LaTeX default style in AASTeX631

Radial Velocity Variability of Hot Jupiter Candidates in TESS

Megan Wilson

ABSTRACT

In an effort to confirm transiting planet candidates detected by the Transiting Exoplanet Survey Satellite (TESS), we used the radial velocity observing method to conduct follow up observations on our vetted candidates. We are focused on Hot Jupiter planets in an effort to better understand their role in the collective composition of extra-solar planets and because of the preference that the RV method has in detecting high mass planets orbiting close in to lower mass stars. The radial velocity method is ideal for conducting ground-based follow up observations on companions detected by transit surveys. Another goal in this is to determine the mass of any confirmed planets in hopes to provide more information about the formation and atmosphere of Hot Jupiter planets.

1. INTRODUCTION

The Transiting Exoplanet Survey Satellite (TESS) uses the transit method to find exoplanets that periodically block part of the light from their host stars. It has surveyed the sky in 26 different sectors in search of exoplanets, and will explore stars that are 30 to 100 times brighter than the stars that the Kepler mission observed (6). Because of the nature of the transit method, we expect TESS to detect hundreds more Hot Jupiter planet candidates. A hot Jupiter is a Jupiter sized planet that orbits close to its star with an orbital period of less than ten days. TESS is designed to detect signals from possible planets, and then scientists will conduct follow-up observations to confirm the nature of the candidate. In confirming these candidates, we hope to gain more information about the population of hot Jupiters in the solar neighborhood.

Though TESS and other transit surveys are great at detecting candidates, they cannot differentiate between a real planet and false positive (not a planet). Hot Jupiters are roughly the same size as a brown dwarf or small star, and when the transit method measure the blocked light from the primary star, there is no way of differentiating the nature of the candidate. Transit surveys can only measure the radius and period of the transiting object, which is why we need to use radial velocity to follow up these surveys.

The radial velocity method allows us to determine the difference between planets and stars because this method allows us to measure the actual mass of the candidate. If we can successfully determine what fraction of a representative sub-sample of hot Jupiters are false-positives, we can apply that result to the entire sample in TESS and make inferences about the Hot Jupiter population.

In this paper, we measure whether four targets are RV variable. Section one briefly describes how we chose our sub-sample of hot Jupiter candidates, and how we chose our four targets. In section two we discuss the instrument and the method of observing targets and reducing their data. This process involves flat fielding and fitting models to deduce a wavelength solution for each night observed. Section three details the derivation of the radial velocity method via the cross correlation function, while section four discusses the results we obtained for each target. Section five comments on the possible influencers of the data, as well as positive results and proposals for more observations.

TOI Number	1780	1645	1420	2121
TIC Number	99834717	184679932	231857016	389900760
Right Ascension	165.167	32.294	322.94	23.5041
Declination	64.964	40.402	66.349	65.5149
Sector	21	18	16	25

Table 1. Important and relevant information on the targets chosen for this project.

2. CANDIDATE VETTING

We observed a total of ten nights, with approximately fifteen targets observed each night. To qualify for follow up observations, we had some criteria that each possible transiting candidate had to pass. It must have a TOI disposition of a planet candidate, have an estimated planet radius of between $4R_E$ and $30R_E$, have a transit depth between 5,000 ppm and 50,000 ppm, a TMag less than 13, come from the Science Processing Operations Center (SPOC) source pipeline, and exist between sectors 15 and 26. With regards to the radial velocity standards, we aimed to observe four or five different spectral types, leaving us ample data for the cross correlation procedure.For this thesis we analyzed the data of four targets, TOI-1420, TOI-1645, TOI-1780, and TOI-2121. TOI-1780 is a confirmed exoplanet discovered in 2018 via both the transit and RV detection methods. It has a mass 1.09±0.09 M_{Jup} and a semi-major axis of 0.0269±0.0010 AU. We chose to look at this target to provide corroborating evidence for the planet and to gain experience in recognizing a true hot Jupiter. We chose to analyze TOI-1645, TOI-2121 and TOI-1420 because of the higher number of visits.

3. DATA REDUCTION

To collect data, we used the Astrophysical Research Consortium (ARC) Echelle Spectrograph (ARCES) on the 3.5 meter telescope at the Apache Point Observatory in New Mexico (APO). This particular instrument is a high resolution, double prism cross-dispersed visible light and echelle grating spectrograph that can observe the entire spectrum of 3200-10000Å on 130 spectral orders. (5) It takes a single exposure on a 2048x2048 SITe CCD with a 1.6 inch slit, and boasts a resolution of R 31,500 and 24 micrometer pixels (3).

3.1. *CCD Reduction*

When observing, we take a series of images that measure the current at an exposure time of zero. The images measure the efficiency of the pixels in the CCD. In the initial step of data reduction, we combined all the images using the statistical median of the array, to create "master" bias, flat, and lamp frames. To create a completely reduced image, we subtract the combined bias image from the science image that was observed.

3.2. *Wavelength Calibration*

The use of Thorium-Argon lamps allows the user to easily extract a wavelength scale for each pixel due to the abundance of emission lines of a Thorium-Argon lamp. This specific lamp is relatively well suited for temperature changes and other factors that may impact imaging. To calculate the wavelength solutions for each order, we a one dimensional Gaussian model to fit each order to a 4th-degree polynomial to map the pixel position of a given wavelength. The wavelength solution for ARCES is susceptible to changes in temperature, pressure, and other environmental factors which may yield the need for us to offset the data ranging from -5 to 8 pixels. Though these wavelength solutions for the Thorium Argon lamps should be consistent, we acknowledge that environmental factors will inevitably show up in our data, which motivates manipulation of some orders. We first adjusted the offset to an appropriate value, and to further adjust the wavelength solutions, we used the Thorium Argon solution to remove lines that contributed to a high RMS number. It was important that we kept at least 5 pixels in each order to ensure accurate results. We manually adjusted bad orders in this manner to achieve a calibration RMS less than 0.01. Once the wavelength solutions were measured and subsequently adjusted, we plotted the spectra.

4. RADIAL VELOCITY DERIVATION

Once the wavelength solution is calculated, we can begin the process to extract the radial velocities. Calculating the radial velocity for each target requires a series of corrections to account for the movement of the Earth and other contributing factors. The overall goal is to the use the cross correlation technique to extract the most precise measurement. We first choose the RV standard, then cross correlate the two, and finish with applying the corrections.

4.1. *Radial Velocity Standards*

To begin this process, we observed and compared Radial Velocity standards of known stars to consider as candidates for the cross correlation relationship. In choosing the Radial Velocity Standard, we compared the spectra of both stars for all orders on the same graph, and analyzed the lines. To determine if an RV standard was a good fit, we looked at each order and its prominent lines, searching for similarities in both frequency of variations and intensity of lines. For every prominent line in the target spectra, we looked for a matching signal in the standard observed

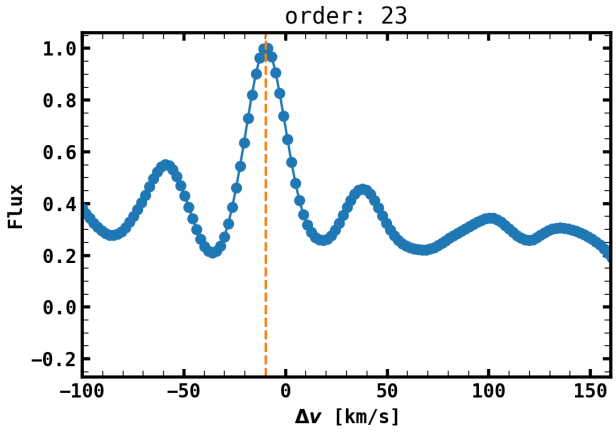

Figure 1. This figure shows an example of the telluric lines that we see on our cross correlation plots. It is a result of interference from absorption lines in the Earth's atmosphere, and is due to the ground-based nature of spectrographs. These somewhat vary depending on the location of the instrument and the conditions of the environment at the time, but are almost always present in these observations.

took the images of about eleven RV standards, hoping for a wide variety of possible cross correlation companions. We compared the spectra of each target star with all eleven standards in order to ensure the best match possible. The standard fit three of our chosen targets was HD111484B, and the other was HD173701. Their spectral types are G0V and G8V respectively. The range of wavelengths at which we viewed the spectra varied from about 4000 Angstroms to 7000 Angstroms, the range decreasing in wavelength with respect to increasing order number. Once we chose the RV standard that best matched our target's spectrum, we began to cross correlate.

4.2. *Cross Correlation*

With the cross correlation method, we measure the similarity in peaks of two arrays as a function of the displacement of one relative to the other. We first continuum-normalize the spectra by applying and dividing out a median filter with a window of 201 points. We then re-sample each spectrum into a logarithmic wavelength space using a linear interpolation to ensure that each point is a constant velocity offset. The velocity offset is calculated by

$$\frac{\lambda_i - \lambda_{i+1}}{\lambda_i}$$

Each spectrum is then transformed into a new flux using the transformation

$$F_{new} = 1 - F_{norm}$$

at which point we start the cross correlation, which is represented by the summation

$$C_i = \sum_k T_k S_{k+i}$$

(1) where C is the new array.A strong cross correlation function has a singular, defined peak centered at the radial velocity measurement for each order. At lower orders, from about twenty to thirty, we can see the affects telluric lines in the cross correlation function. To get a measured radial velocity value, we averaged the radial velocities determined by the cross correlation function for each order in the spectra. In accounting for barycentric correction, we corrected for the effects of the Earth's rotation and precession, as well as the motion of the observatory towards the target. The equation that represents this correction is

$$v_{true} = v_{measured} - v_{barycentric} - \frac{v_{measured} v_{barycentric}}{c}$$

5. RESULTS

In the following section we will provide and elaborate on our results from applying our reduction and analysis to each of our four chosen targets.

5.1. *TOI-1780*

We only observed TOI-1780 on the night of April 8th, 2021. With only one visit we cannot confidently determine the validity of a planet, but we still wanted to conduct the data reduction and analysis for the purpose of gaining experience with spectra of a confirmed transiting planet. We measured the true radial velocity on the night of observation to be 3.07 ± 0.48 km/s. The cross correlation function yielded well-defined peaks for orders that do not succumb to

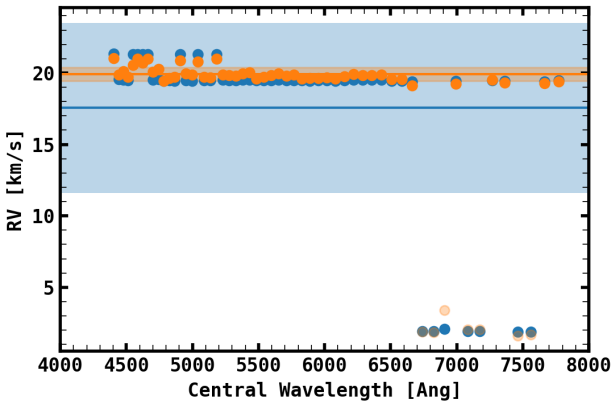

Figure 2. Figure 2 shows the cross correlation function for order 54 on the night of April 8th 2021 for TOI-1780. There is a clear peak at which the peak radial velocity is identified and marked by the dotted orange line. We see little to no interference from other signals at the base of the graph, which supports to planet nature of the confirmed candidate.

atmospheric interference, and do not appear to have any interrupting signals from other sources, which is a good sign when trying to vet out other companions, such as a binary. Compared to the other targets that we observed,

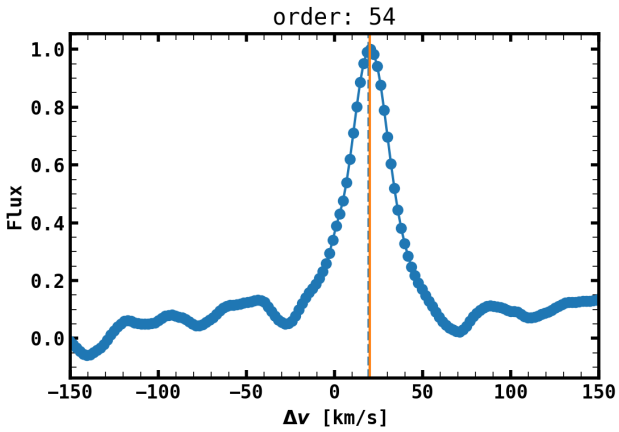

Figure 3. This graph represents the measured peak radial velocity at each order for the target TOI-1780. There is clearly a larger error present here, along with telluric presence at the larger wavelenghts. There are more of these for this observation, which was conducted on April 8th, 2021. The error represented in this graph measured out to be 0.48 km/s, which is not large enough to suspect other signals at play, yet is also not low enough, thus we assume there were other forces that contributed to this, such as intrumental or measuring errors.

TOI-1780 had a greater amount of what seems to be atmospheric effects, which can be shown in the distribution of radial velocities. The wavelength solution for this particular night of observation was relatively good, and did not require a manual pixel offset. For the cross correlation function, we used the RV standard hd111484B. This planet is confirmed as KPS-1b orbiting a K1 type main sequence star, with a planet mass of $1.09 M_{Jup}$ and a planet radius of $1.03 R_{Jup}$ (2).

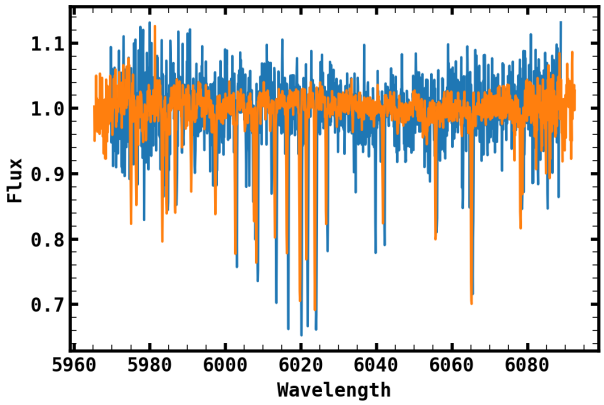

Figure 4. Here we see the spectral comparison of RV standard hd111484B and the target TOI-1780 at order 54. The orange spectra is the RV standard, while our target is displayed through the bluw spectra. This is a great spectral match, as confirmed by the prominent lines of both spectra, as well as the consistency in the magnitude of such lines. This may be the only target that we observed which has spectral lines longer than those of its corresponding RV standard.

5.2. *TOI-1645*

This transiting candidate had four visits between November 2020 and January 2021. We also used the RV standard hd111484B across all four observing nights for our cross correlation. The spectra of the two stars matched relatively well, confirming that the errors we see in this data are not necessarily due to a bad RV standard match.

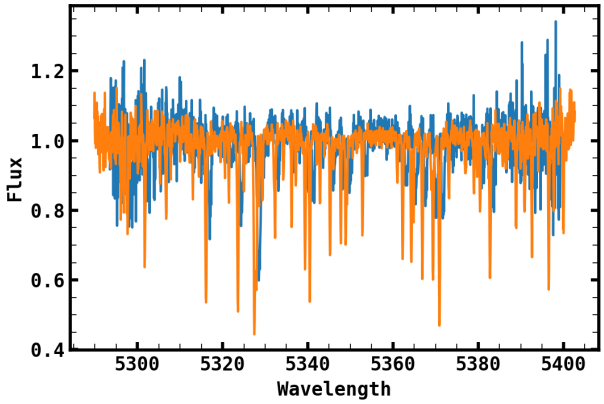

Figure 5. This is the compared spectra of the RV standard hd111484B and the target TOI-1645 at order 54. The blue spectrum represents the target star, and the orange represents the RV standard. We see similar prominent lines from both spectra, and it is clear that the signal from the RV standard is stronger in the length of its lines compared to the target star. Again, the length of the lines does not interfere with the cross correlation, we just want to see the same lines originating from a similar position.

In the cross correlation analysis we noticed a large amount of double peaks on higher orders through all visits, indicating that this was not a result of atmospheric interference. On orders that did not have an obvious double peak, the peak was not defined, and had structure that caused it to be misshaped and asymmetric, an early indicator that this target may not be a planet.

In addition, there was a lot of variation in the measured radial velocity of most orders, leading to high error values. The dates that we observed this target are November 6th and 11th of 2020, December 10th of 2020, and January 7th 2021. The unusually high estimated errors in the radial velocity measurements for each visit are 9.87, 12.69, 7.27, and 11.77 km/s respectively.

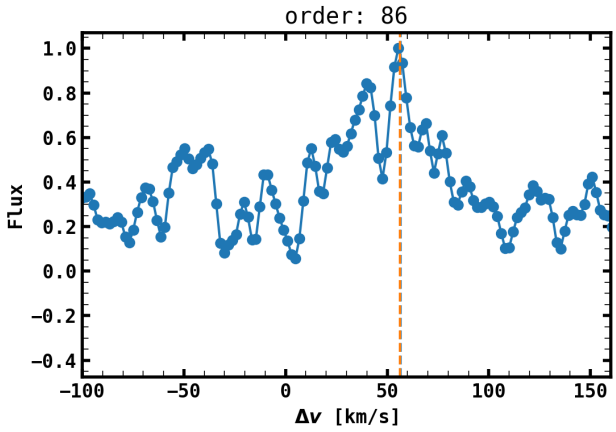

Figure 6. Here we see the cross correlation at order 86 for TOI-1645. Though this is a higher order, we still see lots of interference from other strong signals, and there is a slightly smaller but clear double peak to the left of the higher peaked radial velocity. The dotted orange line represents the measured peak radial velocity. The presence of a double peak in the manner signified to us that this target was an SP2.

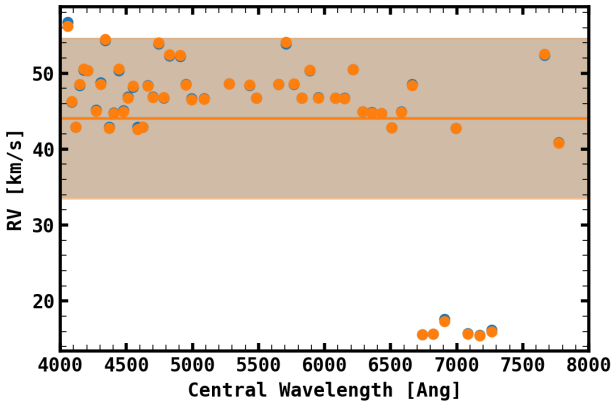

Figure 7. This figure displays the measured peak velocity for each order in the cross correlation function. This distribution confirms our thoughts that the target TOI-1645 is an SP2. The variation in the distribution of radial velocities yields a high error, this night being January 07th 2021, and has an error of 11.77 km/s. High errors in measurements such as this are an indicator of an SP2. We see the same telluric measurements appear in the higher end of the central wavelength measurements, but this is normal throughout all of our observations.

The true radial velocity measurements also varied greatly, and even fluctuated 20 km/s in just five days. True transiting planets will not have this drastic variation in radial velocities in this short amount of time. Given this high error and lack of unity in RV measurements, we have concluded that this is not a transiting planet, but an SP2.

5.3. *TOI-1420*

The candidate TOI-1420 had three visits on November 11th 2020, December 10th 2020, and January 7th 2021. We also used the RV standard hd111484B for the cross correlation process. Like other targets, there were telluric lines that were present in the lower orders of the cross correlation graphs, but were not present in the higher orders. Given that this is occurrence is consistent with the other data, we concluded that they do not have any impact in determining the nature of the candidate. The peaks in the cross correlation were well-defined and consistent at the peak radial velocity, though there existed some minor asymmetry at the base of the peaks.

The distribution of radial velocities were less variant than those observed for TOI-1645, and still showed the same atmospheric effects for approximately five orders, demonstrating consistency in the instrument. After averaging the

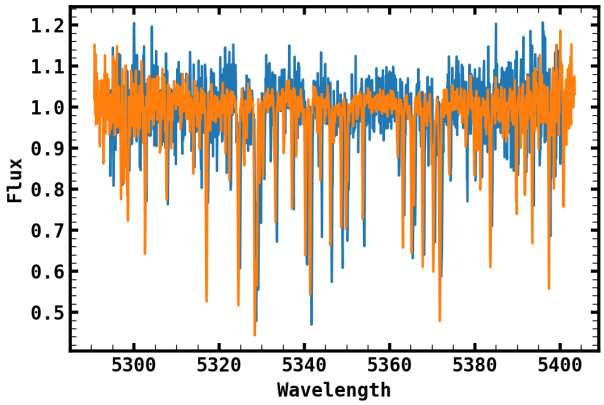

Figure 8. This figure represents the spectra of the RV standard and the target compared on the same wavelength scale at the target TOI-1420. This represents the best matching order in the sequence, order 54. We see the same prominent lines in both spectra. The orange lines represent the spectrum of the RV standard, and the blue represent the spectrum of the target. We see that the RV standard has slightly longer lines, but this does not affect the cross correlation.

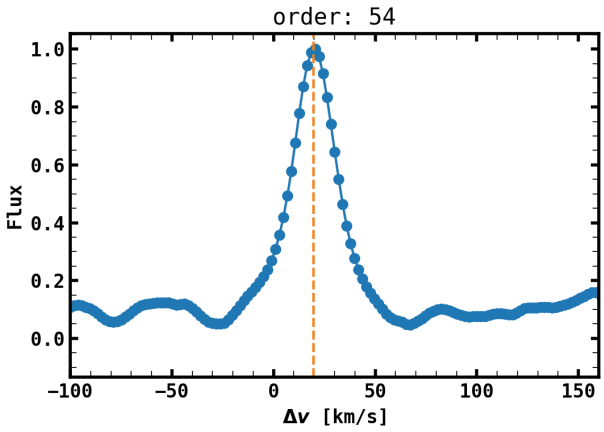

Figure 9. This image is an example of the resulting peaks of the cross correlation function for TOI-1420. We see a well-defined peak and a smooth base, indicating that there were no underlying signals. The orange dotted line represents the measured velocity at the peak.

measured radial velocities for each order and accounting for the necessary barycentric corrections, we obtained true radial velocities of 16.89±0.14, 11.07±0.60, and 22.79±0.73 km/s for the target in order of the nights observed.

We expect the errors to be between 100 and 200 meters per second, and although the calculated errors for this set of data is much lower than those measured for the previous target, two of the three are higher than our desired threshold. This result does not rule out a transiting planet possibility, but it does raise some questions regarding the consistency of the instrument, the nature of the candidate, or the analysis method used. The radial velocities are also more varied than a normal transiting planet, but again, follow up analysis is needed. To follow up, we plotted the different true radial velocities for each night against their corresponding Barycentric Julian Date times, and fit a sine curve for those points. We also used the period measured by TESS to plot the radial velocities against the predicted orbital phase which should also produce a similar sine curve if the candidate is a transiting planet. Unfortunately, the dates on which we observed this candidate proved to be within the same orbital phase, leaving us with not enough data to make an accurate conclusion. Though the sine fit for the radial velocities against Barycentric Julian Date (BJD) was not consistent, more observations are needed.

5.4. *TOI-2121*

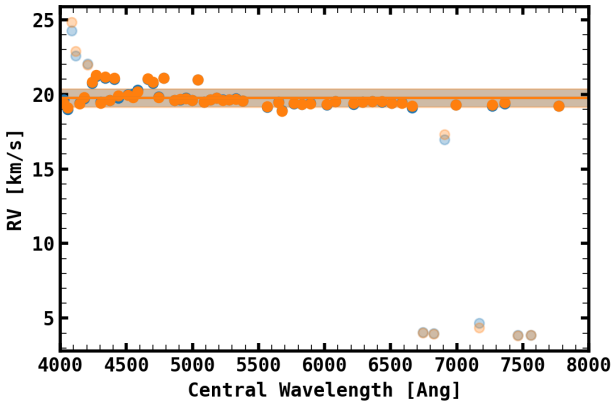

Figure 10. Here we see the radial velocity distribution of the RV's measured at each order for TOI-1420. At lower and higher wavelengths we see non uniformity, along will the telluric interference at lower measured RVs and higher wavelengths. The error in this measurement is 0.139 km/s.

We also observed TOI-2121 on three different occasions, November 6th and 11th of 202, and April 10th 2021. This particular candidate was different from the rest because the target star is very dim. This was also the only candidate in which we used a different RV standard, yet still in the spectral type. The spectrum of standard hd173701 fit much better with the spectrum of this target. We saw more drastic atmospheric effects with a possible double peak at orders of 26 and 27, but we decided that this was not enough information to immediately write this candidate off for a possible planet. Order 34 is where the hydrogen alpha line is most prominent, and we can see this in the cross correlation

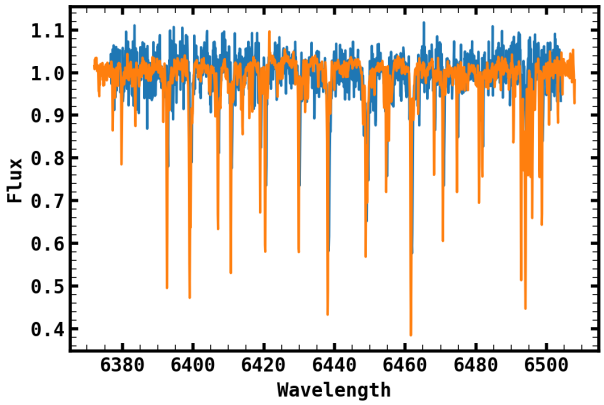

Figure 11. TOI-2121 is the only target where we used a different RV standard, which is hd173701. This particular target was harder to fit, as it had a low SNR value, and many of our observed RV standards have higher SNR and therefore a greater length of their spectral lines. The blue spectra is that of TOI-2121, and the orange is the spectra of our RV standard. There is not much offset in the spectra; they line up well and have similar prominent lines, and this example is at order 36.

through a less defined peak, however, this target did not exhibit this behaviour, and had a peak that was similar to those at higher orders. This could also be due to the low SNR. As the orders progressed higher, the cross correlation peaks became less defined, and some had an indication of interference on the left side. When we averaged the radial velocity measured at the peak of each order's cross correlation, there was little variation in the distribution, aside from the usual atmospheric interference at very low velocities. The true radial velocities that we extracted are 19.09±0.75, 38.00±0.70, and 27.158±0.14 km/s in the order that they were observed. This target has more glaring but similar issues to TOI-1420. The five day gap in observing yields a 20 km/s gap in measured radial velocities, something that is very uncommon for transiting planets. Also, two of the three calculated errors are higher than the threshold that

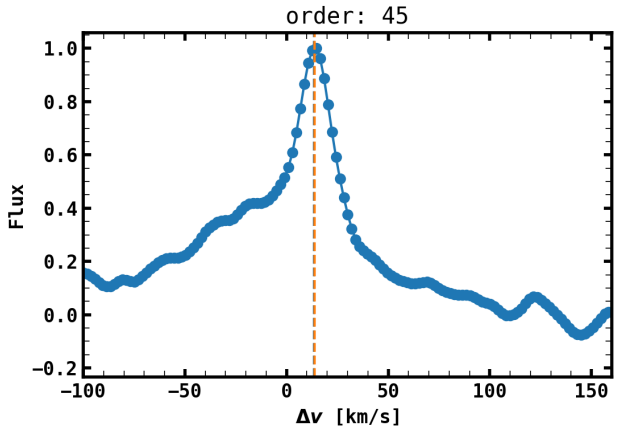

Figure 12. Figure 11 is an example of a cross correlation function at order 45, with the peak radial velocity represented by the dotted orange line. The peak is still somewhat obvious and defined, but it is much less defined than other targets we observed with a higher SNR. There is more interference on the left side, and this behavior is consistent throughout the entire range of orders.

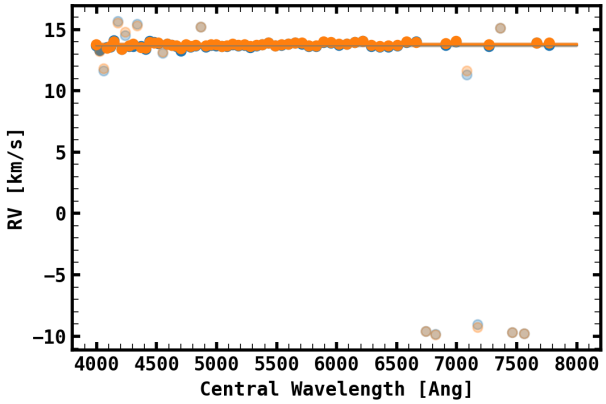

Figure 13. This image shows us the radial velocity distribution of the peak radial velocities measured at each roder of the cross correaltion function. We see the normal five tellruic liens at higher wavelengths, with little variation in the radial velocity measurements. The data represented in this graph and in the other visuals for this target are drawn from the night of April 10th 2021. The calculated error for this night is 0.14 km/s, and is the lowest of all the errors for this target.

we deemed acceptable. To look further into the possibility of a planet, we conducted the same analysis as with the previous target, and looked at the sine curves that the radial velocity produces. The days that we observed were in the same orbital period, which does not give us any helpful information that would aid in determining the validity of its status as a planet. The graph of radial velocity for each night against its measured BJD did not produce a pleasant sine curve, but more data would be needed to confirm anything.

6. CONCLUSIONS

From the analysis of the data, we have a previously confirmed planet, and SP2, and two planet candidates that require more follow up visits in order to determine the nature of the transit. Three visits for a target is just barely enough to create a sine fit if the data exists in different orbital phases. The two remaining candidates, TOI-1420 and TOI-2121, have demonstrated good quality data and have not given us any indication that they are anything other than planets. Their candidacy as a transiting planet cannot be confirmed nor denied from the analysis that we have done so far, but passing this initial test is a step in the positive direction. We are also satisfied with successfully identifying a false-positive in TOI-1645.

6.1. *Proposal for Follow-Up*

To get more information for the purpose of either confirming or denying the existence of a planet, we must have more data in different orbital phases. It would also be ideal to have at least four more visits for each target in ensure good quality data. Another goal is to determine the mass of the confirmed exoplanets. In addition to the original science goal of this paper, determining such masses would help in the field of Hot Jupiter formation and assist in classifying the atmospheres of these planets. To find the mass of an exoplanet, we use the standard radial velocity equation

$$v_{star} = \frac{m_p sin(i)}{M_{star} + m_p} \sqrt{\frac{G(M_{star} + m_p)}{a}}$$

(4) where G is the gravitational constant, m_2 is the companion mass, m_1 is the mass of the host star, and a is semi-major axis, which can also be substitued with the proper transformation for orbital period. From TESS data we have access to the orbital period and the mass of the star, and our radial velocity measurements will put us in a position to determine the mass of the transiting planet candidate. The inclination angle of a planetary system can be hard to determine, as not all systems are aligned with us, setting a limitation of this technique.

6.2. *Potential Inhibitors*

As we previously mentioned, the vulnerability of the instrument to weather changes may lead to variation in the instrument. The most obvious issue to us the the variability in the wavelength solution from night to night, demonstrated by a pixel offset ranging from -5 to 8. Two main observing nights in November had offsets of the range mentioned above. Such a drastic change in just a few days can affect the data and create inconsistencies in measurements, which may have a ripple effect as we go further into our derivations. Unfortunately, the only thing that we can do is adjust for the changes and observe on as many nights as possible to create an abundance of potentially good data. A possible effect of this is inconsistency in the same RV standards. This could result in cross correlation peaks being off, and thus returning an inflated or deflated measured radial velocity value, which could account for the differences in radial velocity measurements for objects TOI-2121 and TOI-1420. Accounting for this would be a helpful step to include in follow up analysis, and it may even be productive to take more images of RV standards in the G spectral type, as those have had the best match with this set of data historically. Some error may also be caused by the centering of the star in the slit of the echelle. If the star that is being observed is smaller than the size of the slit, the instrument is unevenly illuminated, which causes the slit image to shift to either side. This percieved shift can translate to a difference in measured radial velocity.

REFERENCES

[1]Carlos Allende Prieto, 2007, Velocities From Cross-Correlation: A Guide For Self-Improvement, The Astronomical Journal, 134:1843–1848

[2]Artem Burdanov et. al, 2018, KPS-1B: The First Transiting Exoplanet Discovered Using An Amateur Astronomer's wide-field CCD Data, PASP

[3]"ARC 3.5m: ARCES." ARC 3.5m ARCES, www.apo.nmsu.edu/arc35m/Instruments/ARCES

[4]Wei, Jason W. May 9, 2018. "A Survey of Exoplanetary Detection Techniques."

[5]Wang, Shu-i. et al, "ARCES: an echelle spectrograph for the Astrophysical Research Consortium (ARC) 3.5m telescope."

[6]"ARC 3.5m: ARCES." ARC 3.5m — ARCES, www.apo.nmsu.edu/arc35m/Instruments/ARCES/.